TURBULENT KINETIC ENERGY BUDGET AND DISSIPATION IN THE WAKE OF 2D OBSTACLE. ANALYSIS OF THE K-eps CLOSURE MODEL

H Gamel, P. Salizzoni, Lionel Soulhac, P. Mejean, Massimo Marro, N. Grosjean, B. Carissimo

Proceedings of the ASME 2014 4th Joint US-European Fluids Engineering Division Summer Meeting and 11th International Conference on Nanochannels, Microchannels, and Minichannels
FEDSM2014
August 3-7, 2014, Chicago, Illinois, USA

FEDSM2014-21489

TURBULENT KINETIC ENERGY BUDGET AND DISSIPATION IN THE WAKE OF 2D OBSTACLE. ANALYSIS OF THE K-ε CLOSURE MODEL

H.Gamel[1]*, P.Salizzoni[1], L.Soulhac[1], P.Méjean[1], M.Marro[1], N.Grosjean[1],
[1] Laboratoire de Mécanique des Fluides et Acoustique - UMR 5270 CNRS –
Ecole Centrale de Lyon - France

B.Carissimo[2]
[2] Centre de Recherche en Environnement Atmosphérique– EDF R&D Ecole Nationale des Ponts et Chausses - France

ABSTRACT

The prediction of the flow dynamics produced by the interaction between a sheared turbulent flow and a bluff body has important implications in the domain of the wind engineering and for what concerns the simulation of atmospheric dispersion of air-born pollutants.

In this study we present the results of the experimental investigation of the flow dynamics in the wake of a 2D obstacle, immersed in a neutrally stratified boundary layer flow. Measurements are performed by means of two different techniques, namely Laser Doppler Anemometry and Stereo-Particle Image Velocimetry. These allow us to map the spatial evolution of the velocity statistics up to their third order moments.

The study focuses in particular on the budget of the turbulent kinetic energy (t.k.e.) and the estimate of its mean dissipation rate. The experimental data-set is the basis for a detailed analysis of the reliability and the main limitations of a classical k-ε closure model.

INTRODUCTION

Even though the increasing performances of computational fluid dynamics (CFD) nowadays permit to run Large Eddy Simulations of a wide variety of environmental flows, the large majority of the CFD studies of pollutant dispersion in industrial and urban sites are currently performed with Reynolds Averaged Navier-Stokes (RANS) models.

In recent years, several studies ([1] [2] [3]) have enlightened the limitations of RANS models in predicting flow and dispersion in regions characterized by a strong imbalance between production and dissipation of the turbulent kinetic energy. A classical example is given by the wake of a bluff body, immersed in a turbulent boundary layer.

The errors in the prediction of the t.k.e. budget terms have a direct impact on the estimates of the turbulent viscosity ν_t, and therefore on the turbulent diffusivity of a passive scalar.

The analyses of the performances of RANS models mainly rely on the comparison of predicted and measured values of means velocities and of the turbulent kinetic energy *k* levels. However, as far as we are aware, almost no study focus on the discrepancies between the modeled and measured values of the t.k.e. dissipation rate ε, since its experimental estimate is difficult to achieve.

The aim of this study is to provide a detailed experimental estimate of the velocity statistics around a 2D obstacle immersed in a turbulent boundary layer, whose thickness δ is about six times the obstacle height H.

In particular, we focus on the terms composing the t.k.e. budget, including its rate of dissipation ε. Their direct experimental estimate allows us to analyze the reliability of the k-ε closure model.

The study is performed experimentally, by means of different measurement techniques, namely Laser Doppler Anemometry (LDA) and Stereo-Particle Imagery Velocimetry (S-PIV).

In what follows, we first define the quantities involved in the t.k.e. budget and the different experimental methods used to estimate ε. We then recall the basic relations of the k-ε model.

Once presented the experimental set-up and techniques, we discuss our results concerning the characterization of the flow in the incoming boundary layer impacting the obstacle and in its wake. We end by discussing the agreement between our experimental results and a k-ε closure model.

TURBULENCE KINETIC ENERGY BALANCE

Assuming a statistically steady state and incompressible flow, the t.k.e. budget can be expressed as:

$$\overline{u_j}\frac{\partial k}{\partial x_j} = \underbrace{-\overline{u_i'u_j'}\frac{\partial \overline{u_i}}{\partial x_j}}_{P} - \underbrace{\frac{1}{2}\frac{\partial \overline{u_i'u_i'u_j'}}{\partial x_j}}_{\nabla\cdot T} - \underbrace{\frac{1}{\rho}\frac{\partial \overline{p'u_i'}}{\partial x_i}}_{\Pi} + \underbrace{\nu\frac{\partial}{\partial x_j}\left[\overline{u_i'\left(\frac{\partial u_i'}{\partial x_j}+\frac{\partial u_j'}{\partial x_i}\right)}\right]}_{D} - \varepsilon \quad (1)$$

where ν and ρ are the kinematic viscosity and density, p is the pressure, u_i is the fluid velocity component in the x-direction and ε represents the mean dissipation rate of t.k.e., defined as

$$\varepsilon = \nu\left(\overline{\frac{\partial u'_i}{\partial x_k}\frac{\partial u'_i}{\partial x_k}}\right) \quad (2)$$

The correct prediction of the terms composing the t.k.e. budget represents the basis for the evaluation of the accuracy of second order closure moments [4].

However, it is worth noting that the experimental estimates of some terms of equation (1) are not trivial. For example, the turbulent transfer term ∇·T involves the spatial derivatives of third order velocity correlation, whose estimate requires a large number of samples. The direct measure of ε from the equation (2) is even harder, since it requires a spatial resolution of the (instantaneous) velocity field of the order of the Kolmogorov dissipative scale.

Direct and indirect estimates of ε

In the last decades there have been various studies presenting experimental estimates of ε. Among these we cite the work of of Baldi et al. [5] and Baldi and Yianneski [6] who performed combined PIV and LDA measurements within stirred vessels with a spatial resolution of 0.1mm and that of Michelet et al. [7] who estimated velocity gradients on a 0.5mm length scale by means of a couple of LDA system in a grid turbulence flow.

In both cases the integral length scale of the flow did not exceed 0.1m, so that the experiments could provide an exhaustive mapping of ε in most of the domain. Similar measurements are much more difficult to perform in simulated atmospheric flow, or in other kind of environmental flow, characterized by a higher gap between the Eulerian Length scale and the dissipative Kolmogorov scale.

In these latter flows a mapping of ε can be achieved only by making some simplifying assumptions.

The most adopted assumption concerns the condition of local isotropy of the flow, that leads to a simplification of equation (2) as [8] :

$$\varepsilon_{iso} = 15\nu\overline{\left(\frac{\partial u'}{\partial x}\right)^2} \quad (3)$$

Furthermore, since the direct measure of instantaneous velocity gradients remains a challenge, these are usually estimated invoking the frozen turbulence Taylor's hypothesis:

$$\varepsilon_{iso} = \frac{15\nu}{\overline{u}^2}\overline{\left(\frac{\partial u'}{\partial t}\right)^2} \quad (4)$$

where $\overline{u}$ is the time averaged velocity. It is worth mentioning that equation (4) is reliable only if the turbulence intensity is low, i.e. $\overline{u'^2} \ll \overline{u}^2$.

The same assumption of local isotropy allows ε to be estimated from velocity spectra as

$$\varepsilon_{spectrum} = 15\nu\int \kappa_1^2 E_1(\kappa_1)\,d\kappa_1 \quad (5)$$

where $E_1(\kappa_1)$ is the one-dimensional power spectrum and κ_1 is the wave number.

Alternatively, ε can be evaluated as the residual of the t.k.e. budget. In given dynamical conditions of the flow, some of the terms of equation (1) can be neglected since their order of magnitude is significantly lower than that of the other terms. For example, in case of a high Reynolds number and a low Mach number flow, terms D and Π become negligible so that equation (1) reduces to

$$\overline{u_j}\frac{\partial k}{\partial x_j} = \underbrace{-\overline{u_i'u_j'}\frac{\partial \overline{u_i}}{\partial x_j}}_{P} - \underbrace{\frac{1}{2}\frac{\partial \overline{u_i'u_i'u_j'}}{\partial x_j}}_{\nabla\cdot T} - \varepsilon \quad (6)$$

This approach was adopted by Hussein and Martinuzzi [9] in order to determine ε in the flow around a 3D obstacle by means of a LDA system measuring two velocity components. To that purpose they introduced a series of simplifying assumptions concerning the intensity of the missing velocity component and on its gradients.

In the present case we focus on a simpler flow configuration, characterized by the absence of gradients of the time averaged flow variables in the transverse direction y, so that the t.k.e. budget (6) becomes:

$$\overline{u}\frac{\partial k}{\partial x} + \overline{w}\frac{\partial k}{\partial z} = \left\{\begin{matrix} -\overline{u'u'}\frac{\partial \overline{u}}{\partial x} - \overline{u'w'}\frac{\partial \overline{u}}{\partial z} \\ -\overline{w'u'}\frac{\partial \overline{w}}{\partial x} - \overline{w'w'}\frac{\partial \overline{w}}{\partial z}\end{matrix}\right\} - \frac{1}{2}\left\{\begin{matrix} \frac{\partial \overline{u'u'u'}}{\partial x} + \frac{\partial \overline{u'u'w'}}{\partial z} + \frac{\partial \overline{v'v'u'}}{\partial x} + \\ \frac{\partial \overline{v'v'w'}}{\partial z} + \frac{\partial \overline{w'w'u'}}{\partial x} + \frac{\partial \overline{w'w'w'}}{\partial z}\end{matrix}\right\} - \varepsilon_R \quad (7)$$

where u, v, and w indicates the three velocity components in the direction x, y and z, respectively.

RANS k-ε model

In the k-ε model the Reynolds-averaged momentum equation are closed assuming the classical Boussinesq hypothesis:

$$\overline{u_iu_j} - \frac{2k}{3}\delta_{ij} = -\nu_t\left(\frac{\partial \overline{u_i}}{\partial x_j} + \frac{\partial \overline{u_j}}{\partial x_i}\right) \quad (8)$$

And estimating the turbulent viscosity as

$$\nu_t = C_\mu \frac{k^2}{\varepsilon} \quad (9)$$

where C_μ is a constant. The model is completed by two more transport equations that expresses the budget of the t.k.e. and its dissipation rate. These are usually expressed in closed form by modeling the correlation terms as

$$\frac{\partial k}{\partial t} + \overline{u_j}\frac{\partial k}{\partial x_j} = \frac{\partial}{\partial x_i}\left(\left(\nu + \frac{\nu_t}{\sigma_k}\right)\frac{\partial k}{\partial x_i}\right) + P - \varepsilon \quad (10)$$

were σ_k is a constant. The t.k.e. production P is estimated as:

$$P = \frac{\nu_t}{2}\left(\frac{\partial \overline{u_i}}{\partial x_j} + \frac{\partial \overline{u_j}}{\partial x_i}\right)^2 \quad (11)$$

The ε transport equation is:

$$T = \frac{1}{2}\overline{u'_i u'_j u'_j} = -\frac{\nu_t}{\sigma_k}\frac{\partial k}{\partial x_j} \quad (12)$$

and where ε is computed by

$$\frac{\partial \varepsilon}{\partial t} + \overline{u_j}\frac{\partial \varepsilon}{\partial x_j} = \frac{\partial}{\partial x_i}\left(\left(\nu + \frac{\nu_t}{\sigma_\varepsilon}\right)\frac{\partial \varepsilon}{\partial x_i}\right) + C_{\varepsilon_1} P \frac{\varepsilon}{k} - C_{\varepsilon_2}\frac{\varepsilon^2}{k} \quad (13)$$

The values of the constant introduced in the model are given in table 1.

C_μ	σ_k	σ_ε	$C_{\varepsilon 1}$	$C_{\varepsilon 1}$
0.09	1	1.3	1.44	1.92

Table 1: k-ε constant values.

EXPERIMENTAL SET-UP AND TECHNIQUES

The experiments were performed in the wind tunnel of the Laboratoire de Mécanique des Fluides et d'Acoustique at the École Centrale de Lyon. The test section of this tunnel measures 9m in length, 1m in height and 0.7m in width. To generate a boundary layer with characteristics similar to those of an atmospheric boundary layer, we used a combination of spires [10] [11] at the entrance of the test section (0.5m in height) and roughness blocks at the floor of the tunnel. These were formed by a set of square section bars (1.5cm x 1.5cm) normal to the flow and placed from the beginning of the test section up to a distance of 5H from the 2D obstacle, as shown in fig. 1.

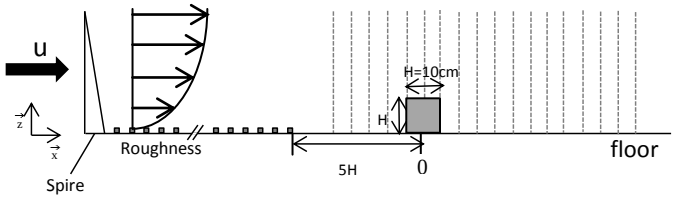

fig. 1: Overview of the wind-tunnel installation. The dotted lines represent the studied area.

With this setup, the height of the boundary layer δ is about 550 mm and the friction velocity to the ground u_*=0.33 m/s. The obstacle has a square section with a side of 0.1m.

Velocity measurements were made with LDA and Stereo-PIV techniques. The LDA equipment consists of an argon fluorescence laser with a power of 5W and of an optical probe with two components. The beams have a diameter of 2.2mm and are spread of about 39mm. Their wave lengths are 488nm and 514.5nm. The frontal lens has a 400mm focal length.
Stereo-PIV measurements were made around the two-dimensional obstacle in the x-z plane (fig. 1). The image resolution is 1280x1024 pixels and the observed areas are about 200x200 mm. For correlated cells, the interrogation window is set to 32x32 pixels with a square shape and a 50% superposition. Each area is constituted with the acquisition of 50 000 pairs of images at a frequency of 4Hz.

EXPERIMENTAL RESULTS

Incoming boundary layer flow

We begin by a sketch of the dynamics of the incoming turbulent boundary layer flow. This was experimentally investigated by means of an LDA system.
Vertical profiles of velocity statistics were recorded within the test section at a distance of approximately 8 times the height of the vortex generators placed at its entrance.
At that distance the flow has reached a dynamical equilibrium and can be considered as homogeneous in the x-y plane.
Figure 2 shows the vertical evolution of some of the key parameters of the flow in non-dimensional form: namely the mean velocity deficit, the standard deviation of the three velocity components (σ_u, σ_v and σ_w), the Reynolds stress (and the turbulent viscosity. The second order statistics are compared to profiles presented by Raupach and al [12] and collected within boundary layers developing over wall with various roughness.
Generally, the statistics of the two data sets are in good agreement. The main discrepancies can be observed for σ_u whose values generally exceed those presented by Raupach and al [12].
In Figure 3 are presented the vertical profiles of the t.k.e. dissipation rate, provided by the different methods. The estimate ε_R obtained as a residual of equation (6) shows good agreement with that provided by the isotropic relation, both through the time dependent signals, ε_{iso}, and its Fourier transform, $\varepsilon_{spectrum}$. For completeness we have also plotted the evolution of ε given by the assumption of a local dynamical equilibrium, as predicted by the similarity theory, i.e.:

$$\varepsilon_{th} = \frac{u_*^3}{z\kappa} \quad (14)$$

where κ is the Kàrmàn Constant.

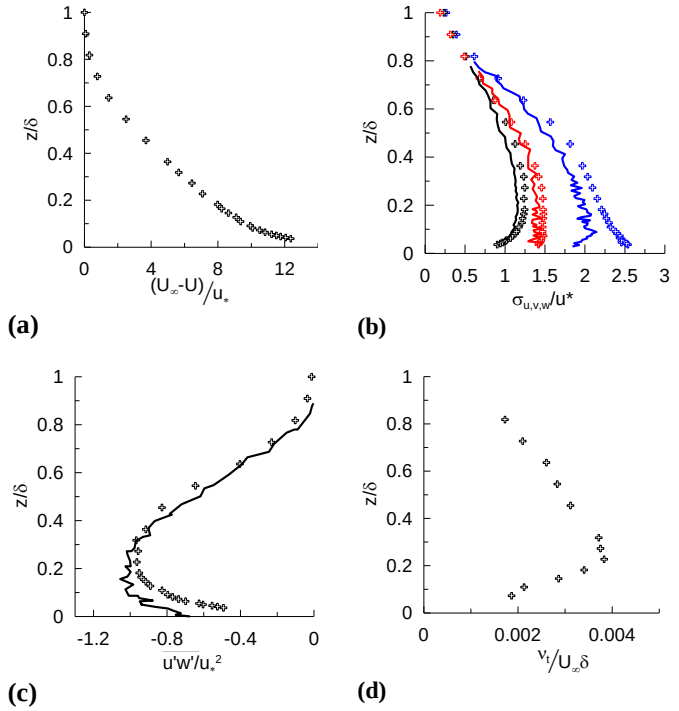

fig. 2: Velocity statistics within the incoming boundary layer flow. The lines in figure (b) and (c) refers to data by Raupach and al [12]. In figure (b) the blue color represent σ_u/u_*, the red color represent σ_v/u_* and the black color σ_w/u_*

This estimate is quite in good agreement in the lower part of the boundary layer and close to its upper boundary; however it differs significantly in the core of it.

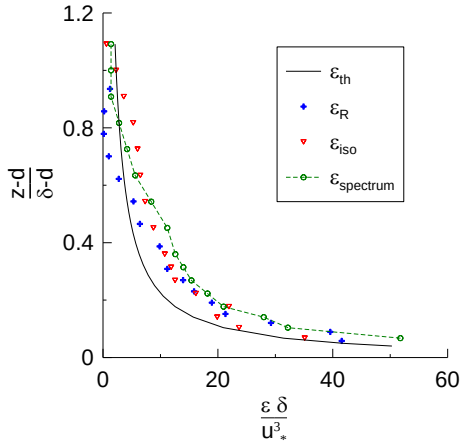

fig. 3: Comparison of different estimates of ε in the incoming boundary layer.

FLOW IN THE WAKE OF A 2D OBSTACLE

Comparison with previous results

Before examining the flow statistics in the wake of the 2D obstacle we compare profiles of first and second order moments of the velocity components obtained by previous authors [13] by means of a PIV system in a similar experimental configuration. The comparisons are presented in figure fig. 4 and fig. 5 and show velocity profiles registered at a distance of 4H from the obstacle.

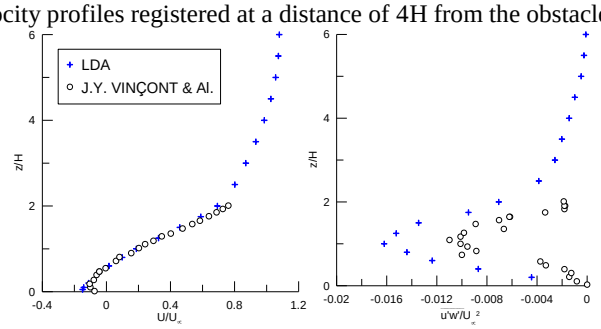

fig. 4: Vertical profiles of mean velocity and Reynolds stress at x=4H, comparison between the current study and Vinçont and al. [13].

We can notice that our results show generally good agreement with those of Vinçont et al. [13]. The slight differences that can be observed may be due to two main features: the differences in the Reynolds numbers (in our case Re=210000 instead of Re=70733) and a different wall roughness.

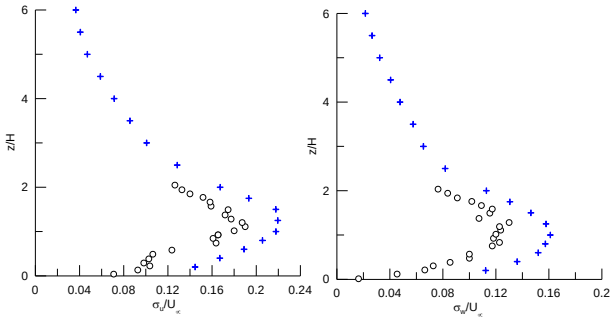

fig. 5 : Standard deviations of the longitudinal and vertical velocity at x=4H. Comparison with Vinçont et al. [13].

Comparison between LDA and Stereo-PIV

We have performed velocity measurements by means of two experimental techniques. The Stereo-PIV system provided measurements of all three components whereas the LDA provided the longitudinal and vertical velocity components only.

Vertical profiles of mean and standard deviation of the longitudinal and vertical velocity, as well as of their correlation are presented in fig. 6-10.

These show a remarkably good agreement between LDA measures and Stereo-PIV measures. The only slight discrepancies can be observed in the upper part of the profile of the vertical mean velocity W at x=1.5H (fig. 7).

From the mean velocity profiles we can easily infer the existence of a recirculating region developing downwind the obstacle, that extends up to a distance of about 6H. The peak of the velocity standard deviations appears slightly higher than the obstacle height. This is due to the existence of a recirculating bubble taking place over the obstacle roof, that shifts upward the shear mixing layer between the recirculating region and the

external flow. This is also shown by the profiles of the Reynolds stress ((10)), that exhibits a peak at about 1.4H.

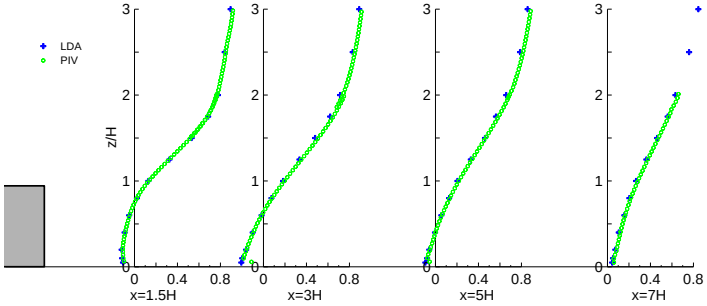

fig. 6: Longitudinal mean velocity U/U_∞

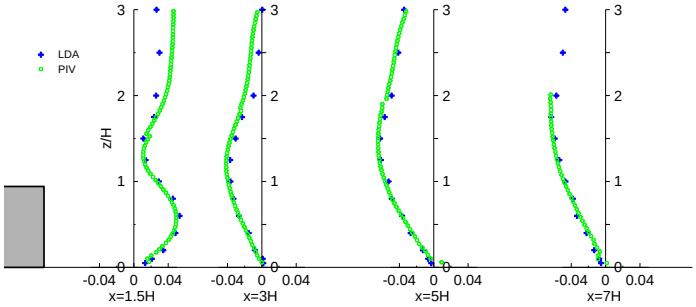

fig. 7: Vertical mean velocity W/U_∞

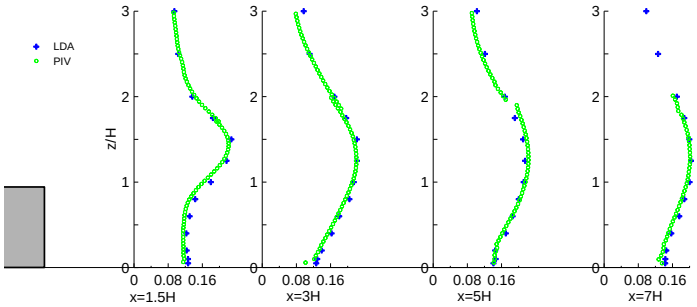

fig. 8: Longitudinal velocity standard deviation σ_u/U_∞

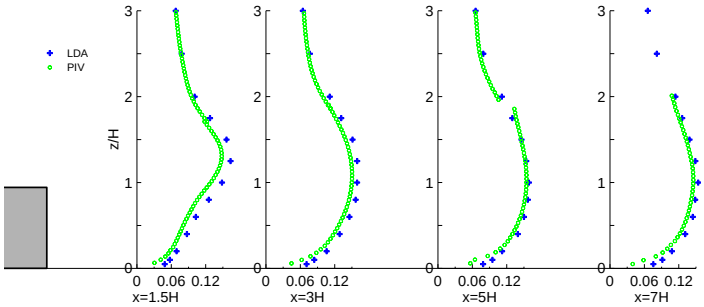

fig. 9: Vertical velocity standard deviation σ_w/U_∞

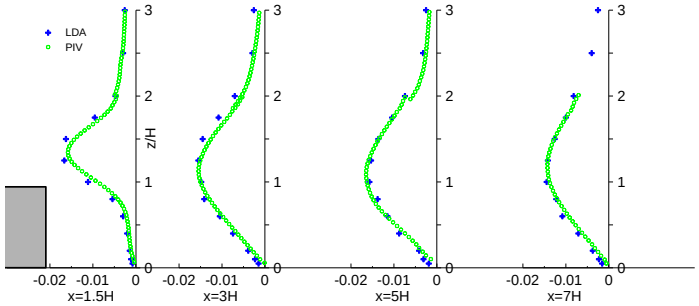

fig. 10: Reynolds stress: $\overline{u'w'}/U_\infty^2$

From the analysis of mean velocity and Reynolds stress we can infer by means of equation (7) an experimental estimate of the turbulent viscosity ν_t, whose profiles are plotted in fig.11. These show that ν_t is almost constant in the vicinity of the obstacles and that its values tend to increase in the far wake. In order to show more directly the effect of the presence of a bluff body in the incoming turbulent flow, we have then analyzed the difference of ν_t registered upwind and downwind the obstacle, $\Delta\nu_t = \nu_t^{down} - \nu_t^{up}$. These profiles (fig. 12) clearly show that close to the obstacle, the increased level of the Reynolds stress (fig. 10) does not correspond to a higher efficiency in the turbulent transfer of momentum.

As fig. 12 shows, the value of ν_t at x=1.5H are even lower than those observed upwind the obstacles. An increased effectiveness of the turbulent momentum transfer is achieved only moving further on downstream the obstacle.

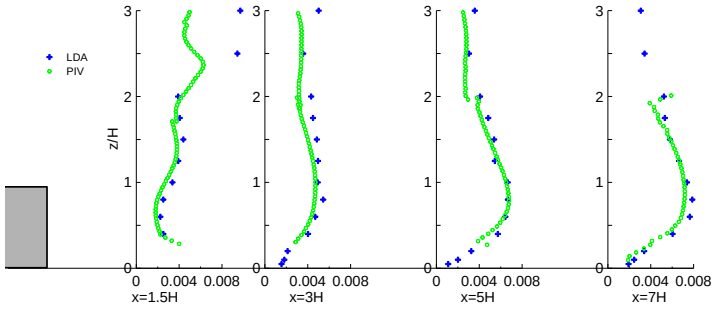

fig.11:Turbulent viscosity: $\nu_t/(\delta\, U_\infty)$

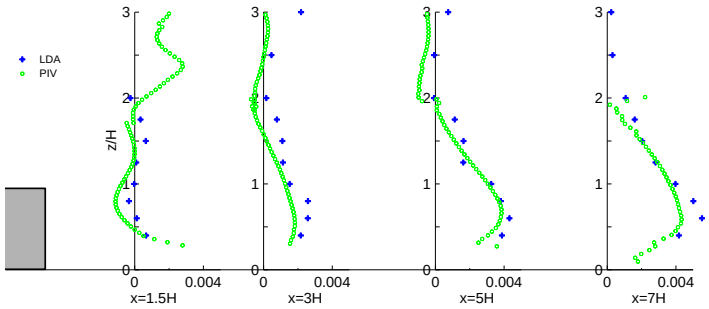

fig. 12: $\Delta\nu_t/(\delta\, U_\infty)$

A further analysis concerns the spatial evolution of the mean dissipation rate of t.k.e. ε, estimated as the residual of equation

(7). It is worth mentioning that the LDA measurements do not allow us to fully characterize the turbulent transfer term *T* in the t.k.e. budget (eq. 6) since they do not provide any information on the contribution of the transversal velocity fluctuations. In order to evaluate the error induced by neglecting the terms containing the fluctuations of the transversal velocity, i.e. v', we have estimated their relative contribution on the total turbulent transfer T. As it is shown in fig. 13 this contribution reaches a maximum of about 20% at a height of about 1.5H, in the core of the shear mixing layer, and close to the downstream edge of the obstacle, i.e. x=1.5H and x=3H. In the rest of the velocity field its contribution can be considered almost negligible.

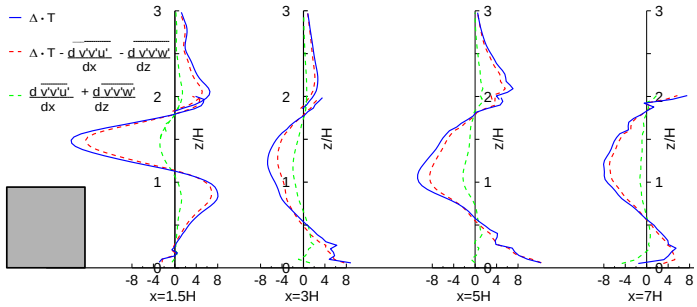

fig. 13: Influence of the transversal velocity component v' in the turbulent transport term T. Transport with all terms is the blue line, without v' component is the red dotted line and only the terms include the v' component is the green dotted line.

Neglecting these contributions has therefore a direct impact on the estimates of ε provided by the LDA measurements, compared to those given by PIV measurements, only in a very limited region of the flow. The main differences between the two estimates can be observed at x=1.5H and close to z=1.5H, where ε exhibits a peak, whereas in the rest of the flow they show a rather good agreement (fig. 14).

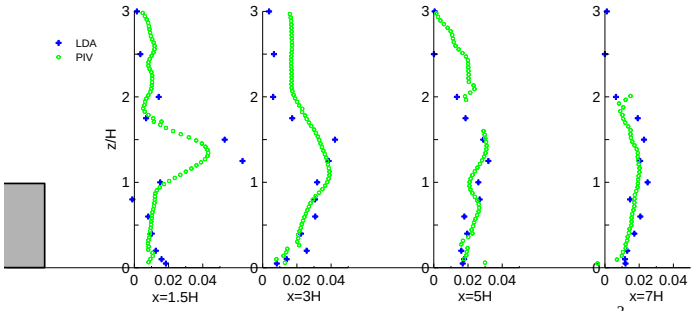

fig. 14: Dissipation rate of turbulent kinetic energy: $\varepsilon\delta/U_\infty^3$

Confrontation of the different TKE budget terms between experimental measurements and standard k-ε model

Finally we present a preliminary analysis of our data set aiming in evaluating the consistency of some of the basic assumption adopted in a standard k-ε model.

In particular we focus on the reliability of the equation (8) and (12) and namely on the values of the coefficient C_μ and σ_k.
In fig. 15 we have determined the value of the coefficient C_μ, as directly estimated by our experimental data, i.e. as:

$$C_\mu = \frac{\varepsilon \nu_t}{k^2} \qquad (15)$$

As fig. 15 shows, the value of the coefficient C_μ is highly dependent on the different regions of the velocity field. Even though the linear regression passing from the origin provides C_μ= 0.081, the data show a non negligible scatter and significant discrepancies from the reference value 0.09 adopted in k-ε standard model.
Conversely the experimental estimates of σ_k (fig. 16) are much less scattered with a best fit value of 0.9, which is very close to that usually adopted in the literature.

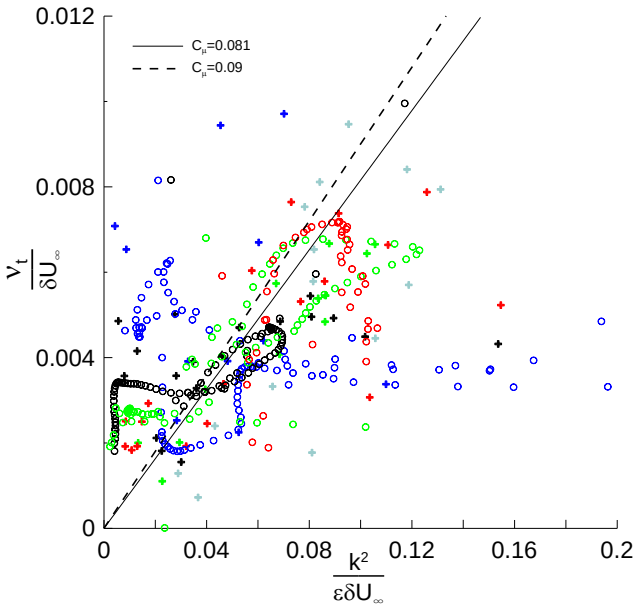

fig. 15: Experimental determination of C_μ. The cross (+) represents the LDA measurements and the circle (o) represents the Stereo PIV measurements. The dark-blue color is the position x=1.5H, the black is x=3H, the green is x=5H, the red is x=7H, and the light blue is x=8.5H

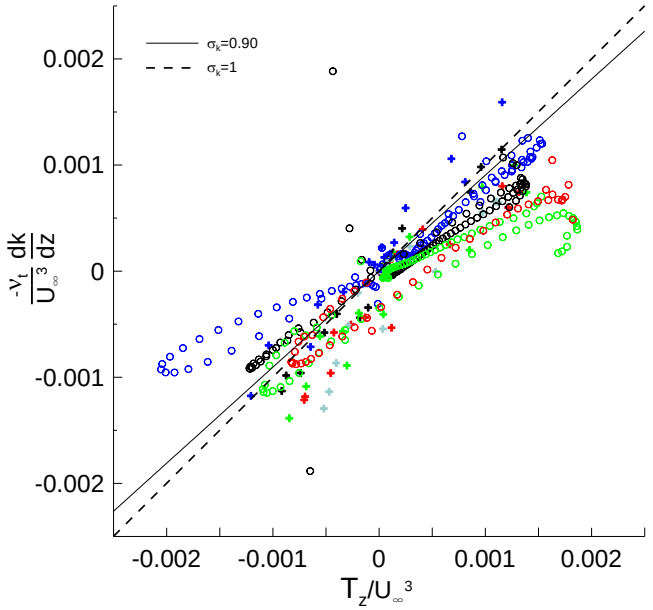

fig. 16: Experimental determination of σ_k The cross (+) represents the LDA measurements and the circle (o) represents the Stereo PIV measurements. The dark-blue color is the position x=1.5H, the dark is x=3H, the green is x=5H, the red is x=7H, and the light blue is x=8.5H

CONCLUSION AND PERSPECTIVES

This study presents some preliminary results of the experimental investigation of the flow past a 2D obstacle immersed within a neutral atmospheric boundary layer. Measurements are performed with an LDA and stereo-PIV system providing estimates of the velocity statistics, up to their third order moments. These allow us to directly infer the magnitude of the terms composing the t.k.e. budget equation and therefore to estimate the t.k.e. dissipation rate as a residual of this same equation. These experimental estimates are the basis for the analysis of the accuracy of second order closure models that are widely used in the simulation of atmospheric flows. Further analysis will concern the estimates of the integral length scales and they link with the local values of turbulent viscosity and diffusivity. The same experimental configuration will also be used to evaluate the dynamics of the dispersion of a passive tracer emitted at ground level source upwind and downwind the 2D obstacle.

ACKNOWLEDGMENTS

The authors would like to thank EDF (Électricité de France) for its contribution and support to this project.

REFERENCES

[1] A. Mochida, Y. Tominaga, S. Murakami, and R. Yoshie, "Comparison of various k-εmodel and DSM applied to flow around a high-rise building - report on AIJ cooperative project for CFD prediction of wind environment," *Wind & Structures*, vol. 2-4, pp. 227-244, 2002.

[2] "Comparison of LES and RANS calculations of the flow around bluff bodies," *Journal of Wind Engineering and Industrial Aerodynamics*, vol. 69-71, pp. 55-75, 1997.

[3] Z. Xie and I.P. Castro, "LES and RANS for turbulent flow over arrays of wall-mounted obstacles," *Flow Turbulence Combust*, vol. 76, pp. 291-312, 2006.

[4] S. B. Pope, *Turbulent Flows*, 10th ed., Cambridge University Press, Ed., 2000.

[5] S Baldi, A Ducci, and M. Yianneski, "Determination of Dissipation Rate in Stirred Vessels Through Direct Measurement of Fluctuating Velocity Gradients," vol. 27-3, no. 275-281, 2004.

[6] S Baldi and M Yianneski, "On the quantification of energy dissipation in the impeller stream of a stirred vessel from fluctuating velocity gradient measurements," *Chemical Engineering & Technology*, vol. 59-13, pp. 2659-2671, 2004.

[7] S Michelet, Y Antoine, F Lemoine, and M Mouhouast, "Mesure directe du taux de dissipation de l'énergie cinétique de turbulence par vélocimétrie laser bi-composante : validation dans une turbulence de grille," *Comptes rendus de l'Académie des sciences.*, vol. 326, pp. 621-626, 1998.

[8] Karman and Howarth, "On the Statistical Theory of Isotropic turbulence," *Proceedings of the Royal Society London*, vol. 164A, 1938.

[9] H.J. Hussein and R.J. Martinuzzi, "Energy balance for turbulent flow around a surface mounted cube placed in a channel," *Physics of Fluids*, no. 8, pp. 764-780, 1995.

[10] J Counihan, "An improved method of simulating an atmospheric boundary layer in a wind tunnel," *Atmospheric Environment*, no. 3, pp. 197-214, 1969.

[11] HPAH Irwin, "The design of spires for wind simulation," *Journal of Wind Engineering and Industrial Aerodynamics*, no. 7, pp. 361-366, 1981.

[12] M.R. Raupach, R.A. Antonia, and S. Rajagopalan, "Rough-wall turbulent boundary layers," *Applied Mechanics Reviews*, vol. 44, no. 1, pp. 1-25, 1991.

[13] J.Y. Vinçont, S. Simoëns, M. Ayrault, and J.M. Wallace, "Passive scalar dispersion in a turbulent boundary layer from a line source at the wall and downstream of an obstacle," *JFM*, vol. 424, p. 127, 2000.

[14] D Poggi, G Katul, and J Albertson, "Scalar dispersion within a model canopy : Measurements and three-dimensional Lagrangian models," *Advances in Water Resources*, vol. 29-2, pp. 326-335, 2006.